Available online at www.sciencedirect.com

ScienceDirect

journal homepage: www.elsevier.com/locate/he

Hydrogen diffusion through Ru thin films

O. Soroka [a], J.M. Sturm [a,*], C.J. Lee [b], H. Schreuders [c], B. Dam [c], F. Bijkerk [a]

[a] Industrial Focus Group XUV Optics, MESA+ Institute for Nanotechnology, University of Twente, P.O. Box 217, 7500 AE Enschede, the Netherlands

[b] Fontys Institute of Engineering, De Rondom 1, 5612 AP Eindhoven, the Netherlands

[c] Materials for Energy Conversion and Storage (MECS), Department of Chemical Engineering, Faculty of Applied Sciences, Delft University of Technology, Van der Maasweg 9, 2629 HZ Delft, the Netherlands

HIGHLIGHTS

- Hydrogen diffusion through Ru films was studied.
- Optical monitoring in transmission is used, with Y as H sensitive layer.
- Pd capping layer ensures that H diffusion through Ru is limiting for H transport.
- Diffusion constant and activation energy obtained in range 25–100 °C.

GRAPHICAL ABSTRACT

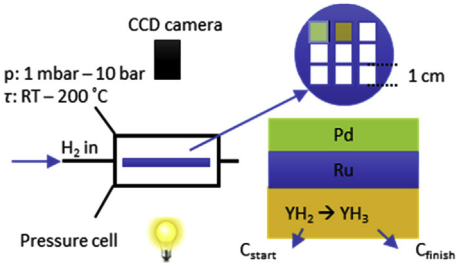

ARTICLE INFO

Article history:
Received 7 November 2019
Received in revised form
20 March 2020
Accepted 25 March 2020
Available online 17 April 2020

Keywords:
Hydrogen diffusion
Ruthenium
Yttrium
Optical transmission
Activation energy

ABSTRACT

In this paper, an experimental measurement of the diffusion constant of hydrogen in ruthenium is presented. By using a hydrogen indicative Y layer, placed under the Ru layer, the hydrogen flux through Ru was obtained by measuring the optical changes in the Y layer. We use optical transmission measurements to obtain the hydrogenation rate of Y in a temperature range from room temperature to 100 °C. We show that the measured hydrogenation rate is limited mainly by the hydrogen diffusion in Ru. These measurements were used to estimate the diffusion coefficient, D, and activation energy of hydrogen diffusion in Ru thin films to be $D = 5.9 \times 10^{-14}$ m^2/s · exp (-0.33 eV/$k_B\tau$), with k_B the Boltzmann constant and τ the temperature.

* *Corresponding author.*
E-mail address: j.m.sturm@utwente.nl (J.M. Sturm).

https://doi.org/10.1016/j.ijhydene.2020.03.201

Introduction

Due to hydrogen induced embrittlement and corrosion of materials [1], development of a diffusion barrier for hydrogen is crucial for applications such as nuclear fusion technology [2–4], equipment for space applications [5], hydrogen storage [6], construction materials in the oil/gas industry [7] and protection of optical elements for soft X-ray and extreme ultraviolet optics [8]. Ru is often studied as protective layer or material, since it is relatively inert, while having a lower atomic mobility compared to more noble metals as Au and Ag, due to its relatively high melting temperature. In addition, the catalytic properties of Ru enhance the possibility to clean oxide and carbon contamination by atomic hydrogen [9–13].

However, hydrogen transport in Ru has been poorly studied in comparison to other materials: to our knowledge, there are no studies reported on hydrogen diffusion in Ru. Although molecular hydrogen dissociatively adsorbs on clean Ru (0001) surfaces [14], the heat of solution of hydrogen in Ru is positive [15], indicating that H does not readily dissolve in bulk Ru. This low bulk solubility makes Ru a good candidate as diffusion barrier for hydrogen. There are many techniques (Neutron Scattering, Solid State Nuclei Magnetic Resonance, Elastic Recoil Detection Analysis etc.) that allow the hydrogen content and distribution in a metal film to be quantified, but they are high-cost, not easily accessible, potentially destructive for the investigated sample or not applicable for low hydrogen concentrations in metal [16–18]. Ideally, a technique that allows direct comparison of hydrogen transport in different metals, which can also work with both atomic and molecular hydrogen sources needs to be developed.

An alternative to directly sensing hydrogen is to infer hydrogen transport via changes in material properties. Yttrium (Y) is highly sensitive to hydrogenation, forming di- and trihydrides, which causes a metal (Y and YH_2) to insulator (YH_3) transition. The hydrogenation of a Y film can be easily detected optically, for instance, with the hydrogenography technique. Hydrogenography is a method that enables rapid measurement of the change in optical transmittance of a film due to hydrogen absorption [19]. First, hydrogen dissolves in the Y lattice forming an α-phase and then the transition to the YH_2 phase starts. When formation of YH_2 is complete, the second transition to YH_3 takes place. Both transitions, Y-YH_2 or YH_2-YH_3, occur consecutive resulting in a two-phase mixture at any given moment during Y hydrogenation. According to the Beer-Lambert law, the change in transmittance depends exponentially on hydrogen concentration for such a two-phase system. Thus, after applying a scaling factor to the transmittance, the changes in hydrogen concentration in Y can be readily obtained. Although hydrogenography only provides a relative measure of hydrogen content, the measurements can be implemented *in situ*, which allows the hydrogenation rate of a Y film to be obtained. The hydrogenation rate may be used for estimation of hydrogen diffusivity in Ru.

It was demonstrated that Y films can be used for measuring the hydrogen lateral mobility in metal films [20]. We here propose to use a trilayer stack for hydrogen diffusion studies through thin Ru films, similar to the structure used in a previously reported Mg_2Ni hydrogenation kinetics study [21]. A sketch of the structure is shown in Fig. 1a. A sensing Y layer is covered with a diffusion barrier (Ru film) and a continuous Pd cap is added on the top. The purpose of the Pd layer is to accelerate hydrogen adsorption, protect the material under investigation from oxidation, and dissociate molecular hydrogen. Hydrogen uptake by such a Pd/Ru/Y structure can be monitored by measuring the change in its optical transmittance.

Generally speaking, the hydrogen uptake by Y depends on both surface (ad- and desorption, sticking probability) and bulk (enthalpy of solution, diffusion, interface penetration) processes that hydrogen atoms undergo in the Pd/Ru/Y stack. This complicates the analysis unless one process, such as diffusion through the middle (Ru) layer, is the rate limiting step. Under these conditions, all processes apart from the rate limiting step can be neglected. In this study, a method, demonstrated by Borgschulte et al. [22], was used to distinguish the rate limiting process (under the experimental conditions given below) by measuring the hydrogenation rate at varied hydrogen pressure. It is shown that the hydrogen diffusion through the Ru layer is significantly slower than all other processes, and, therefore, the hydrogenation rate can be attributed to diffusion through Ru.

This allows the diffusion kinetics of hydrogen through thin polycrystalline Ru films to be studied. Assuming a steady hydrogen flux through Ru, the diffusion coefficient and activation energy of hydrogen diffusion in Ru was estimated. The validity of this estimation is further discussed.

Materials and methods

Sample preparation and characterization

In this study, all layered structures were deposited using DC magnetron sputtering in a vacuum system with a base pressure about 10^{-8} mbar. For optical transmission measurements at varied hydrogen pressure, 10 × 10 mm polished quartz (PGO) substrates were used. For the measurements at different temperatures, different kinds of substrates (quartz from three different suppliers, sapphire and $SrTiO_3$ single crystal substrates) were coated with identical Pd/Ru/Y trilayers in the same deposition run. The surface roughness of the deposited samples was measured with AFM (the typical root mean square values are 0.4–0.8 nm for quartz substrates and 0.2 nm for single crystal substrates) before and after loading with hydrogen. No significant roughening upon hydrogenation was detected.

Hydrogenography

Yttrium was chosen as an indicator due to its ability to change optical transmittance during hydrogen absorption. Yttrium forms hydrides with different structural and optical properties. First, the metallic YH_2 phase forms and then the transition to the dielectric YH_3 phase takes place. Measuring changes in the sample transparency during either Y-YH_2 or YH_2-YH_3 transition allows to find the ratio of two phases at every moment of hydrogen loading.

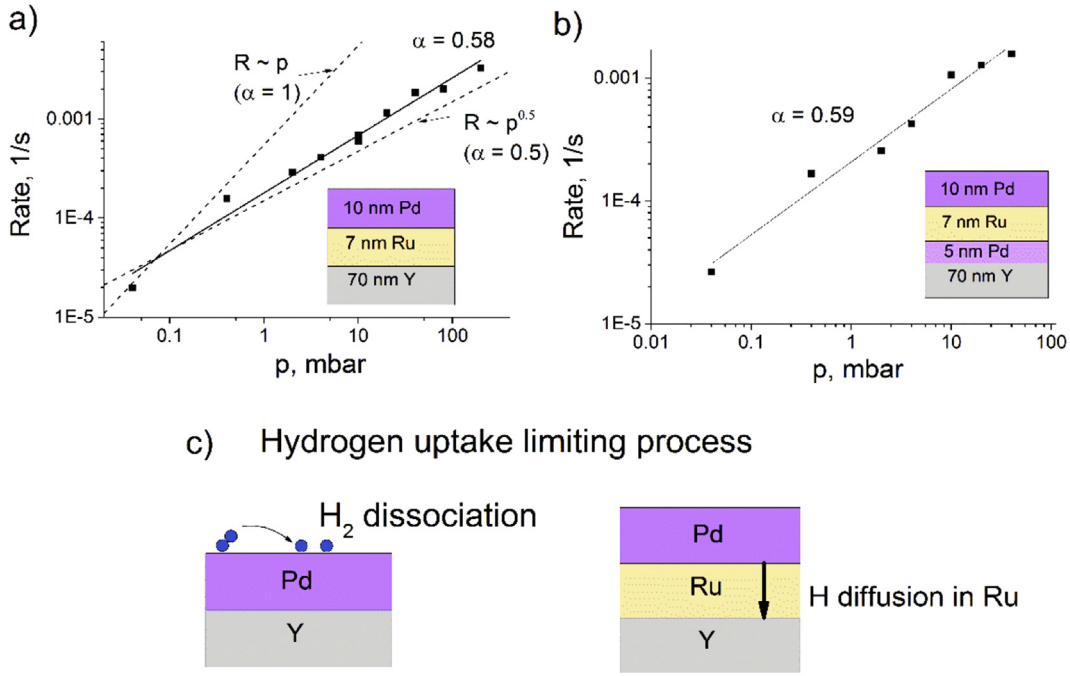

Fig. 1 – The rate of hydrogenation (in terms of a time derivative of $\ln(T/T_0)$) versus the applied hydrogen pressure for Pd/Ru/Y (a) and Pd/Ru/Pd/Y (b) structures on PGO quartz substrates at room temperature. The dashed lines in (a) indicate two extreme cases, when $\alpha = 0.5$ (diffusion limited) and 1 (H_2 dissociation limited); (c) A sketch highlighting the rate-limiting process for samples without and with a Ru layer.

A detailed description of the hydrogenography setup can be found elsewhere [23]. A sample holder enabled simultaneous measurement of up to nine 10 × 10 mm samples. Pure hydrogen gas was used in measurements at different temperatures, while a mixture of 4% H_2 in Ar was used in measurements at varied H_2 pressures. Discrepancies in time needed for the YH_2 phase to form for identical samples was observed during the first loading from Y to YH_3. Therefore, the data from the first cycle of hydrogenation to YH_3 and dehydrogenation to YH_2 was excluded from analysis. The YH_2-YH_3 transition in the following cycles was used for determination of the hydrogenation rate. At higher temperatures the hydrogenation rate was faster than the pressure ramp, which limited the temperature range up to 100 °C.

Results and discussion

Limiting processes for the hydrogenation rate

To identify the limiting step for hydrogen transport in a Pd/Ru/Y trilayer, the pressure dependence of the hydrogenation rate was measured for two structures, Pd/Ru/Y itself and Pd/Ru/Pd/Y (with a spacing Pd layer between Ru and Y), which allows the effect of the Ru/Y interface presence to be investigated. For these measurements, the hydrogenation rate is calculated from a linear fit of the $\ln(T/T_0)$ slope, where T is transmission and T_0 is the initial transmittance before hydrogen loading, when loading the yttrium film from YH_2 to YH_3. The order, α, of the rate dependence on the applied hydrogen pressure $R \tilde{} p^{\alpha}$, indicates whether the hydrogenation rate is limited mainly by surface (H_2 dissociation, $\alpha = 1$) or bulk ($\alpha = 0.5$) processes involved in hydrogen transport to the Y layer. Prior research [22] showed that α is close to unity in a Pd/Y structure and, therefore, hydrogen uptake in this structure is mostly limited by H_2 dissociation on the Pd surface. Here, we find that inserting a Ru layer shifts the power very close to a square root ($\alpha = 0.58$, Fig. 1a), which indicates that the measured rates are mostly limited by the diffusion through Ru (but H_2 dissociation still has small influence). Adding a spacer Pd layer between Ru and Y (Fig. 1b) did not change α significantly, which excludes that the Ru/Y interface in the original trilayer limits the hydrogen transport. Similarly, we assume that the Pd/Ru interface is not rate limiting. From reference experiments performed in our group, it is known that the effective interface width of the Pd-on-Ru interface is 0.7 ± 0.2 nm [24]. Since this is much smaller than the layer thicknesses of the Pd and Ru layers, it is expected that the influence of the Pd layer on hydrogen diffusion inside the Ru layer is negligible. In addition, the reported hydrogen diffusion coefficients at room temperature of 1.9×10^{-15} m^2/s for Pd [25] and 3×10^{-14} m^2/s for Y [26] thin films are 4–5 orders of magnitude larger than the H diffusion coefficient in Ru of 1.9×10^{-19} m^2/s that follows from this work. Thus, it can be concluded that for the test stacks employed in this work, the hydrogenation rate is mainly limited by transport through the Ru film. In view of the much faster H diffusion through Pd and Y, compared to Ru, it is expected that the exact layer thicknesses of Pd and Y will

not affect the measured diffusion kinetics, as long as the Pd film is thick enough to protect the Ru from oxidation.

Hydrogen flux calculation

To estimate the diffusion coefficient of H in Ru, the hydrogen flux should be calculated first. For that, since the change in the optical transmission, T, during the hydrogen loading is attributed to the formation of yttrium hydrides (the transmittance change in the Pd layer is negligibly small and, therefore, omitted), the transmittance is translated into hydrogen concentration x in YH_x. According to the pressure concentration isotherms [27], thermodynamic equilibrium for hydrogen concentrations within the YH_2-YH_3 transition is achieved at a constant (plateau) pressure. The Beer-Lambert law then can be applied within this concentration range. Therefore, the hydrogen concentration, x, is proportional to $ln(T/T_0)$ during the YH_2-YH_3 transition. Assuming that the saturation state corresponds approximately to $x = 2.7$ [28] and a 'shoulder' in the time evolution of transmittance corresponds to $x = 2.1$ (see Supplemental Information), the hydrogen concentration can be calculated for each T value from the initial loading from Y to YH_3 (since the 'shoulder' can be reliably measured only during the first loading). The initial loading from Y to YH_2 is not used for the analysis due to irreversible changes in the film structure. However, the difference between times needed to reach the YH_2 state in a sample without and with a Ru layer is evident in the initial cycle as well (SI).

All further analysis is based on repeated cycles of the YH_2 to YH_3 transition. One such cycle is shown in Fig. 2b. Once the pressure ramp is finished, the H concentration grows linearly with time. Extracting the slope from a linear fit yields the hydrogenation rate of the Y film. Taking into account the thickness of the Y layer, the hydrogen flux can be calculated.

The following non-linear saturation to the YH_3 phase is probably caused by slowing down of the reaction rate due to limited amount of YH_2 [29]. On the other hand, Mooij et al. [30] showed in their study of magnesium hydride that similar behavior happens due to the non-homogeneous nucleation of metal hydride (in our case, nucleation of YH_3).

Diffusion coefficient of hydrogen in Ru

Within the chosen concentration range for cycles, x grows linearly with time (see Fig. 2b). This means that the hydrogen flux throughout the Pd/Ru/Y stack is constant and, hence, Fick's first law can be applied:

$$F = D(\tau)\frac{\partial C}{\partial z}, \tag{1}$$

where F is the hydrogen flux, D is the hydrogen diffusion coefficient in Ru (diffusion in Pd and Y is assumed to be instant), C is the hydrogen concentration distribution along the z-axis (normal to the sample surface). We can assume that $F(\tau) \propto D(\tau)$ only when the concentration gradient is kept constant for all measurements. Let us consider the main factors that influence this concentration gradient. From the top side of the Ru film, there is a concentration of dissolved hydrogen in Pd, C_{Pd}^H. It is constant within one measurement for a given temperature and hydrogen pressure, since equilibrium with H_2 gas is reached much faster than transport through Ru (see Fig. 3a). With Ru having a low hydrogen solubility and forming no hydride [31], the yttrium layer acts like a sink, binding hydrogen as soon as it reaches the Ru/Y boundary due to low chemical potential and fast diffusion of H atom in Y [32,33]. Also, a prior XRD study [34], where no interstitial free hydrogen was detected during the $YH_2 - YH_3$ transition, supports this assumption. Thus, the hydrogen concentration on the Ru/Y boundary can be assumed to be zero. The concentration gradient then only depends on C_{Pd}^H and the thickness of the Ru layer d_{Ru}, which results in a concentration gradient along the z-axis, $\frac{\partial C}{\partial z} = C_{Pd}^H/d_{Ru}$. Taking into account that the concentration $x = C_H/C_Y$, where C_Y is the yttrium atomic concentration, the calculated rate, $R = dx/dt$, can then be used to calculate the hydrogen flux, F, through the Ru film in the following way: $F = RC_Y d_Y$ (d_Y is the Y thickness). Thus, the diffusion coefficient can be estimated as:

$$D(\tau) = \frac{F}{dC/dz} = \frac{C_Y d_Y d_{Ru}}{C_{Pd}^H} R(\tau) \tag{2}$$

We make use of the saturation of hydrogen concentration in palladium to ensure that C_{Pd}^H is kept constant. This is

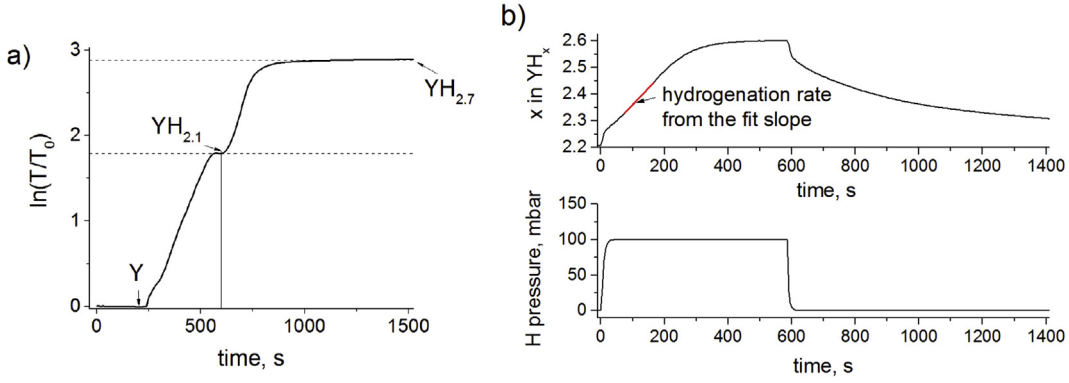

Fig. 2 – (a) The initial loading of Pd/Ru/Y trilayer on quartz (MaTeck) substrate at room temperature. The moment of switching on 1000 mbar of hydrogen coincides with zero of time axis (b) The calculated hydrogen concentration in Y during loading at 100 mbar hydrogen at 40 °C. The bottom subplot shows the H pressure during loading. The pressure ramp leads to a 'jump' of x in the beginning of the top subplot.

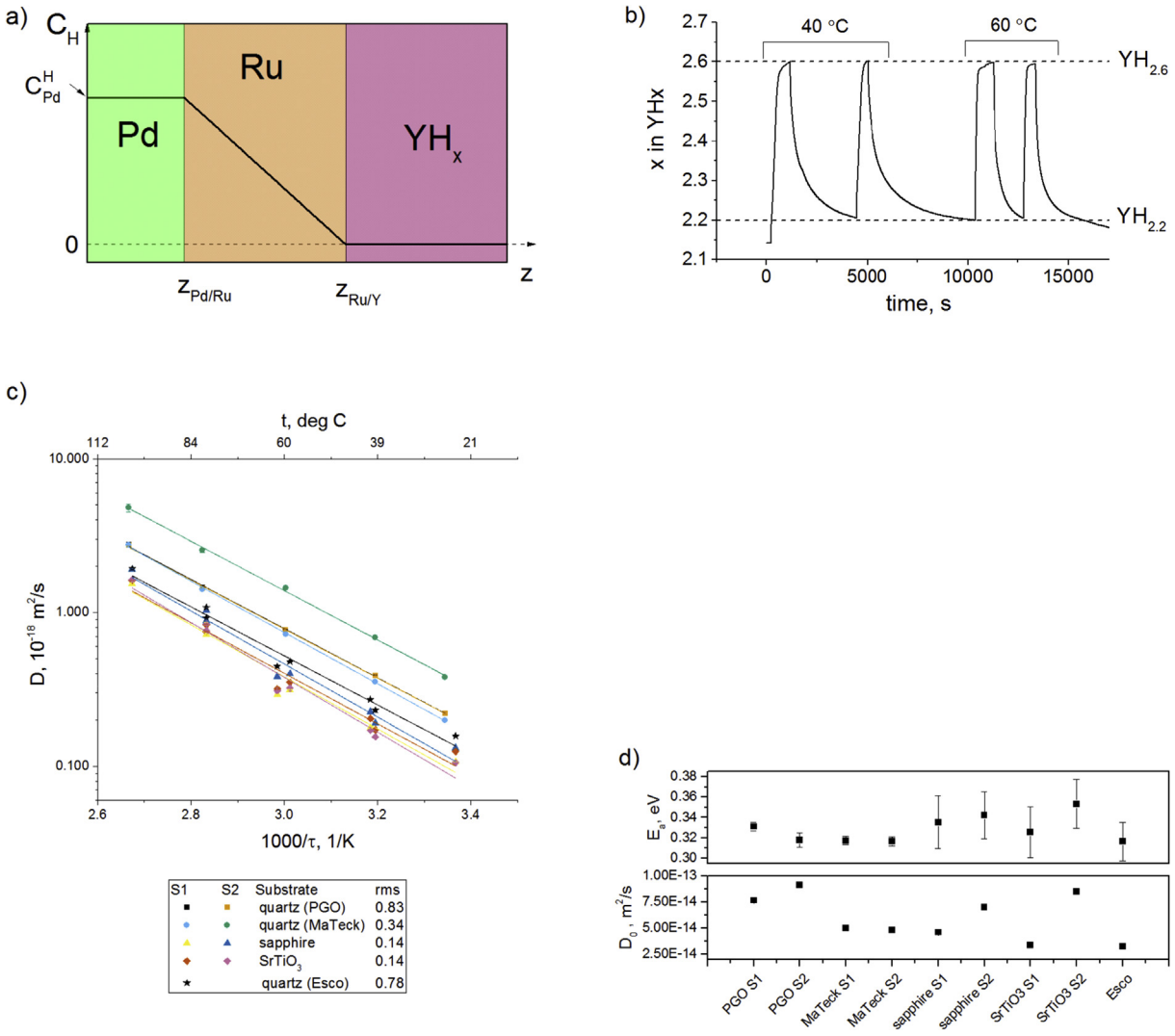

Fig. 3 – (a) A sketch of the Pd/Ru/Y structure and the hydrogen concentration profile in the Ru layer when the steady state regime of the diffusion is achieved: a linear H concentration profile with C_{Pd}^{H} on Pd/Ru and zero on Ru/Y boundary; (b) Loading-unloading cycles at 40 and 60 °C for the S1 sample on a MaTeck substrate; (c) Arrhenius plot for each sample: the diffusion coefficient in Ru (log scale) versus inverse temperature for the same Pd/Ru/Y structure on different substrates (marked with symbol types). The rms roughness derived from AFM scans is indicated for each substrate type in the legend. Different samples within one substrate type are marked with different colors (S1 and S2). The standard error of the data points is smaller than symbol size; (d) The results of a linear fit in (c) for each sample. The error bars correspond to the standard error of the linear fit. (For interpretation of the references to color in this figure legend, the reader is referred to the Web version of this article.)

achieved by using earlier results [35] to set the applied hydrogen pressure such that the final optical transmission corresponds to a fixed value for x ($x = 2.6$). The starting concentration, x, is chosen to be greater than 2.1 to keep the coefficient of the proportionality between the concentration and the intensity ratio the same during the measurements (see Supplemental information). As a result, in these experiments, the hydrogen concentration in yttrium was cycled between $x = 2.2$ and $x = 2.6$ (Fig. 3b).

By measuring the hydrogenation rate for various temperatures, we can estimate the activation energy, E_a, of this diffusion process using the Arrhenius equation $D = D_0 \exp(-E_a/k_B\tau)$, where D_0 is the pre-factor of the diffusion constant, k_B is the Boltzmann constant and τ is the temperature. However, this expression is only valid when the hydrogen diffusion through Ru is the rate limiting step for the entire temperature range. As shown in the previous section, the hydrogen uptake by the Y layer is limited by hydrogen transport through Ru at room temperature. An increase of temperature leads to acceleration of the H_2 dissociation, but the kinetics of the hydrogenation is assumed to remain limited by the Ru layer. On the other hand, higher temperatures lead to a lower equilibrium concentration of hydrogen in Pd. This affects the hydrogen concentration gradient through the Ru layer and complicates the analysis of the diffusion through Ru. To compensate for

this, at each temperature the hydrogen pressure is adapted such that the same hydrogenation state of Y is achieved. In this way, we measure the temperature dependence of the hydrogen transport in Ru with the same driving force.

It is well known that the surface roughness of a substrate can influence the structure of an overlaying thin film. This will also change the rate of diffusion through the layer. In order to understand the influence of the substrate on diffusion, the experiment and calculation described above was performed for several different substrate types. An Arrhenius plot of the diffusion coefficient of hydrogen in Ru is shown in Fig. 3c. Because of the large difference between the data points of identical samples (S1 and S2, Fig. 3c), the fit is performed for each sample separately. Since the largest deviations are observed between identical film stacks on quartz substrates (see the legend of Fig. 3c), we believe that the substrate roughness has an impact on the hydrogen flux. The results of the fit are shown in Fig. 3d. The higher error in the activation energy obtained for sapphire, $SrTiO_3$ and quartz (Esco) samples is due to increased uncertainty in the final hydrogenation state of the yttrium layer ($YH_{2.6}$ for these conditions). This uncertainty is induced by a mismatch between the needed hydrogen pressure to reach $x = 2.6$ and its set value. The average D_0 and E_a over all samples are $5.9 \cdot 10^{-14}$ m^2/s and 0.33 eV.

To check the validity of the used steady state approximation, the hydrogenation times were calculated with a diffusion model, which takes into account the diffusion through the Ru layer only, based on Fick's second law:

$$\frac{\partial C}{\partial t} = D_{Ru}(RT)\frac{\partial^2 C}{\partial z^2}, \tag{3}$$

where $D_{Ru}(RT) = 1.9 \cdot 10^{-19}$ m^2/s, is the diffusion coefficient in Ru at room temperature calculated with obtained D_0 and E_a values. The boundary conditions for the Ru diffusion layer are (Fig. 3a, top):

$$C(z_{Pd/Ru}, t) = C^H_{Pd},\ C(z_{Ru/Y}, t) = 0,$$

with the initial concentration distribution

$$C(z,0) = \begin{cases} C^H_{Pd}, & z = z_{Pd/Ru} \\ 0, & z > z_{Pd/Ru} \end{cases}.$$

Using this model, we can assess the number of accumulated hydrogen atoms in the Y layer as a function of time. According to this calculation, it takes about 80 s to reach 90% of a steady H flux through the Ru layer (i.e. time to establish a linear concentration profile in the Ru layer) and about 1000 s to accumulate enough hydrogen atoms to form the YH_3 phase. Thus, steady state diffusion is reached in the beginning of the whole process, which justifies the use of Fick's first law for diffusion coefficient extraction.

The hydrogen solubility in Ru is expected to be very low and this would change the hydrogen concentration distribution across the Ru layer. As described by Borgschulte et al., the chemical potential of hydrogen (not the concentration) in a multilayer system should be a continuous function [21,32]. When the heat of solution of hydrogen (or the heat of hydride formation) in two layers forming an interface is different, this will result in a sudden change in hydrogen concentration at the interface [32]. The concentration jump at Pd/Ru interface was estimated from the chemical potential equality at the interface (see Pasturel et al. [13]) using the H enthalpy of solution in Ru, +0.55 eV/at H [36] and the enthalpy of formation of palladium hydride, −0.26 to −0.1 eV/at H [21]. The calculated H concentration in Ru is ten orders of magnitude smaller, which would lead to a ten orders higher diffusion coefficient than calculated.

From the other hand, even though the hydrogen concentration in defect-free Ru should be negligibly low, Ru is expected to have a significant H concentration at grain boundaries and defects, since hydrogen readily adsorbs at clean Ru surfaces with coverage up to unity, when exposed to molecular or atomic hydrogen [14,37]. Additionally, the catalytic activity of Ru should be noted [38,39], which can have an impact on hydrogen migration along the grain surfaces. The local H concentration at Ru grain boundaries near the Pd/Ru interface is therefore expected to be similar to the concentration in Pd. If we assume that transport along grain boundaries is the dominating diffusion mechanism, this justifies the usage of $C_{Pd}{}^H/d_{Ru}$ as approximation of the concentration gradient over the diffusion pathways through the Ru film. It has been demonstrated that our 7 nm Ru films are above the threshold thickness for polycrystalline growth [40,41]. We therefore expect that diffusion will be dominated by hopping between defects or transport along grain boundaries. All film stacks in this work were deposited using the same coating procedure, or even produced within the same deposition run. This should give a negligible difference in film thicknesses, although some structure difference may occur due to different roughness of the starting substrate. It should be noted that other Ru deposition methods or Ru thicknesses may lead to a different grain structure, which may result in Ru films with a different diffusion constant from the value reported in this work.

Conclusion

In summary, hydrogen diffusion through a thin Ru film was studied for the first time using hydrogenography on specially prepared multilayer films. Combination of (a) the promotion of H_2 dissociation by a Pd cap and (b) slow permeation in the Ru layer compared to Pd and Y enabled a direct measurement of the hydrogen diffusion rate through Ru. This method can be applied to materials with hydrogen solubilities and diffusivities much lower than in yttrium and Pd. The pre-factor, D_0, of the hydrogen diffusion coefficient of Ru and the activation energy was estimated from loadings at different temperatures and are $5.9 \cdot 10^{-14}$ m^2/s and 0.33 eV, respectively. The main advantage of the presented method for measuring the H diffusion constant through Ru, is that the method provides direct evidence that the measured diffusion rate is limited by diffusion through the Ru film and not by surface or interface processes. In addition, the method can readily be applied to materials that have a low solubility for hydrogen, unlike other common methods as volumetric or desorption measurements.

Acknowledgments

The authors thank Mr. Theo van Oijen for depositing samples. This work is part of the research programme of the Netherlands Organization for Scientific Research (NWO), Domain Applied and Engineering Sciences (AES, previously Technology Foundation STW). The work is additionally supported by Carl Zeiss SMT GmbH (Germany). We also acknowledge the support of the Industrial Focus Group XUV Optics at the MESA + Institute at the University of Twente, notably the industrial partners ASML (the Netherlands), Carl Zeiss SMT GmbH (Germany), Malvern Panalytical (the Netherlands), and the Province of Overijssel (the Netherlands).

Appendix A. Supplementary data

Supplementary data to this article can be found online at https://doi.org/10.1016/j.ijhydene.2020.03.201.

REFERENCES

[1] Dwivedi SK, Vishwakarma M. Hydrogen embrittlement in different materials: a review. Int J Hydrogen Energy 2018;43(46):21603–16. https://doi.org/10.1016/j.ijhydene.2018.09.201.

[2] Xiang X, Wang X, Zhang G, Tang T, Lai X. Preparation technique and alloying effect of aluminide coatings as tritium permeation barriers: a review. Int J Hydrogen Energy 2015;40(9):3697–707. https://doi.org/10.1016/j.ijhydene.2015.01.052.

[3] Zhang G, Wang X, Yang F, Shi Y, Song J, Lai X. Energetics and diffusion of hydrogen in hydrogen permeation barrier of α-Al2O3/FeAl with two different interfaces. Int J Hydrogen Energy 2013;38(18):7550–60. https://doi.org/10.1016/j.ijhydene.2013.03.136.

[4] Zajec B. Hydrogen permeation barrier – recognition of defective barrier film from transient permeation rate. Int J Hydrogen Energy 2011;36(12):7353–61. https://doi.org/10.1016/J.IJHYDENE.2011.03.068.

[5] Corso AJ, Pelizzo MG. Extreme ultraviolet multilayer nanostructures and their application to solar plasma observations: a review. J Nanosci Nanotechnol 2018;19(1):532–45. https://doi.org/10.1166/jnn.2019.16477.

[6] Orimo SI, Nakamori Y, Eliseo JR, Züttel A, Jensen CM. Complex hydrides for hydrogen storage. Chem Rev 2007;107(10):4111–32. https://doi.org/10.1021/cr0501846.

[7] Luo B, Bai P, An T, Zhang S, Wen X, Chen L, Zheng S. Vapor-deposited iron sulfide films as a novel hydrogen permeation barrier for steel: deposition condition, defect effect, and hydrogen diffusion mechanism. Int J Hydrogen Energy 2018;43(32):15564–74. https://doi.org/10.1016/J.IJHYDENE.2018.06.042.

[8] Louis E, Yakshin AE, Tsarfati T, Bijkerk F. Nanometer interface and materials control for multilayer EUV-optical applications. Prog Surf Sci 2011;86(11–12):255–94. https://doi.org/10.1016/j.progsurf.2011.08.001.

[9] Ugur D, Storm A, Verberk R. Kinetics of reduction of a RuO2 (110) film on Ru (0001) by H2. J Phys Chem C 2012;116(110):26822–8. https://doi.org/10.1021/jp309905z.

[10] Li W, Wang H, Jiang X, Zhu J, Liu Z, Guo X, Song C. A short review of recent advances in CO2 hydrogenation to hydrocarbons over heterogeneous catalysts. RSC Adv 2018;8(14):7651–69. https://doi.org/10.1039/c7ra13546g.

[11] Bajt S, Alameda JB, Barbee TW, Clift WM, Folta JA, Kaufmann BB, Spiller EA. Improved reflectance and stability of Mo-Si multilayers. Opt Eng 2002;41(8):1797. https://doi.org/10.1117/1.1489426.

[12] Chen J, Louis E, Harmsen R, Tsarfati T, Wormeester H, van Kampen M, van Schaik W, van de Kruijs R, Bijkerk F. In situ ellipsometry study of atomic hydrogen etching of extreme ultraviolet induced carbon layers. Appl Surf Sci 2011;258(1):7–12. https://doi.org/10.1016/j.apsusc.2011.07.121.

[13] Motai K, Oizumi H, Miyagaki S, Nishiyama I, Izumi A, Ueno T, Namiki A. Cleaning technology for EUV multilayer mirror using atomic hydrogen generated with hot wire. Thin Solid Films 2008;516(5):839–43. https://doi.org/10.1016/J.TSF.2007.06.182.

[14] Kostov KL, Widdra W, Menzel D. Hydrogen on Ru (001) revisited: vibrational structure, adsorption states, and lateral coupling. Surf Sci 2004;560(1–3):130–44. https://doi.org/10.1016/j.susc.2004.04.025.

[15] Griessen R, Riesterer T. Heat OF formation models. Top Appl Phys 1988;63:219–84.

[16] Kirchheim R, Pundt A. Hydrogen in metals. In: Physical metallurgy. 5th ed. 2014. https://doi.org/10.1016/B978-0-444-53770-6.00025-3.

[17] Horinouchi H, Shinohara M, Otsuka T, Hashizume K, Tanabe T. Determination of hydrogen diffusion and permeation coefficients in pure copper at near room temperature by means of tritium tracer techniques. J Alloys Compd 2013;580:S73. https://doi.org/10.1016/j.jallcom.2013.03.293.

[18] Mézin A, Lepage J, Abel PB. Hydrogen permeation properties of molybdenum coatings from absorption-desorption experiments. Thin Solid Films 1996;272(1):132–6. https://doi.org/10.1016/0040-6090(95)06970-4.

[19] Huiberts JN, Griessen R, Rector JH, Wijngaarden RJ, Dekker JP, de Groot DG, Koeman NJ. Yttrium and lanthanum hydride films with switchable optical properties. Nature 1996;380(6571):231–4. https://doi.org/10.1038/380231a0.

[20] Remhof A, Van Der Molen SJ, Antosik A, Dobrowolska A, Koeman NJ, Griessen R. Switchable mirrors for visualization and control of hydrogen diffusion in transition metals. Phys Rev B Condens Matter 2002;66(2):1–4. https://doi.org/10.1103/PhysRevB.66.020101.

[21] Pasturel M, Wijngaarden RJ, Lohstroh W, Schreuders H, Slaman M, Dam B, Griessen R. Influence of the chemical potential on the hydrogen sorption kinetics of Mg 2 Ni/TM/Pd (TM = transition metal) trilayers. Chem Mater 2007;19(3):624–33. https://doi.org/10.1021/cm062157h.

[22] Borgschulte A, Westerwaal RJ, Rector JH, Schreuders H, Dam B, Griessen R. Catalytic activity of noble metals promoting hydrogen uptake. J Catal 2006;239(2):263–71. https://doi.org/10.1016/j.jcat.2006.01.031.

[23] Gremaud R, Broedersz CP, Borsa DM, Borgschulte A, Mauron P, Schreuders H, Rector JH, Dam B, Griessen R. Hydrogenography: an optical combinatorial method to find new light-weight hydrogen-storage materials. Adv Mater 2007;19(19):2813–7. https://doi.org/10.1002/adma.200602560.

[24] Chandrasekaran A, Van de Kruijs RWE, Sturm JM, Zameshin AA, Bijkerk F. Nanoscale transition metal thin films: growth characteristics and scaling law for interlayer formation. ACS Appl Mater Interfaces 2019;11(49):46311–26. https://doi.org/10.1021/acsami.9b14414.

[25] Li Y, Cheng Y-T. Hydrogen diffusion and solubility in palladium thin films. Int J Hydrogen Energy 1996;21(4):281–91. https://doi.org/10.1016/0360-3199(95)00094-1.

[26] Borgschulte A, Lohstroh W, Westerwaal RJ, Schreuders H, Rector JH, Dam B, Griessen R. Combinatorial method for the development of a catalyst promoting hydrogen uptake. J Alloys Compd 2005;404–406:699–705. https://doi.org/10.1016/J.JALLCOM.2005.01.137.

[27] Radeva T, Ngene P, Slaman M, Westerwaal R, Schreuders H, Dam B. Highly sensitive and selective visual hydrogen detectors based on Y_xMg_{1-x} thin films. Sensor Actuator B Chem 2014;203:745–51. https://doi.org/10.1016/j.snb.2014.06.134.

[28] Kremers M, Koeman NJ, Griessen R, Notten PHL, Tolboom R, Kelly PJ, Duine PA. Optical transmission spectroscopy of switchable yttrium hydride films. 1998.

[29] Atkins P, de Paula J. Physical chemistry. 8th ed. New York: W. H. Freeman and Company; 2006.

[30] Mooij L, Dam B. Nucleation and growth mechanisms of nano magnesium hydride from the hydrogen sorption kinetics. Phys Chem Chem Phys 2013;15(27):11501–10. https://doi.org/10.1039/C3CP51735G.

[31] Mueller WM, Blackledge JP, Libowitz GG. Metal hydrides. 5th ed. New York: Academic Press; 1968.

[32] Borgschulte A, Gremaud R, Griessen R. Interplay of diffusion and dissociation mechanisms during hydrogen absorption in metals. Phys Rev B Condens Matter 2008;78(9):94106. https://doi.org/10.1103/PhysRevB.78.094106.

[33] Kuzovnikov MA, Tkacz M. Synthesis of ruthenium hydride. Phys Rev B 2016;93(6):64103. https://doi.org/10.1103/PhysRevB.93.064103.

[34] Soroka O, Sturm JM, van de Kruijs RWE, Makhotkin IA, Nikolaev K, Yakunin SN, et al. Hydrogenation dynamics of Ru capped Y thin films. J Appl Phys 2019;126:145301. https://doi.org/10.1063/1.5094592.

[35] Pivak Y, Schreuders H, Slaman M, Griessen R, Dam B. Thermodynamics, stress release and hysteresis behavior in highly adhesive Pd–H films. Int J Hydrogen Energy 2011;36(6):4056–67. https://doi.org/10.1016/j.ijhydene.2010.12.063.

[36] McLellan RB, Oates WA. The solubility of hydrogen in rhodium, ruthenium, iridium and nickel. Acta Metall 1973;21(3):181–5. https://doi.org/10.1016/0001-6160(73)90001-1.

[37] Hofman MS, Wang DZ, Yang Y, Koel BE. Interactions of incident H atoms with metal surfaces. Surf Sci Rep 2018;73(4):153–89. https://doi.org/10.1016/j.surfrep.2018.06.001.

[38] Noyori R, Hashiguchi S. Asymmetric transfer hydrogenation catalyzed by chiral ruthenium complexes. Acc Chem Res 1997;30(2):97–102. https://doi.org/10.1021/ar9502341.

[39] Morris RH. Exploiting metal–ligand bifunctional reactions in the design of iron asymmetric hydrogenation catalysts. Acc Chem Res 2015;48(5):1494–502. https://doi.org/10.1021/acs.accounts.5b00045.

[40] Müller R, Ghazaryan L, Schenk P, Wolleb S, Beladiya V, Otto F, Kaiser N, Tünnermann A, Fritz T, Szeghalmi A, et al. Growth of atomic layer deposited ruthenium and its optical properties at short wavelengths using Ru(EtCp)2 and oxygen. Coatings 2018;8(11):413. https://doi.org/10.3390/coatings8110413.

[41] Soroka O, Sturm JM, van de Kruijs RWE, Lee CJ, Bijkerk F. Control of YH_3 formation and stability via hydrogen surface adsorption and desorption. Appl Surf Sci 2018;455:70–4. https://doi.org/10.1016/j.apsusc.2018.05.134.